CHEMICAL ENGINEERING TRANSACTIONS
VOL. 86, 2021
A publication of AIDIC
The Italian Association of Chemical Engineering
Online at www.cetjournal.it
Guest Editors: Sauro Pierucci, Jiří Jaromír Klemeš

**ISBN** 978-88-95608-84-6; **ISSN** 2283-9216

# Heating strategies in cellulose pyrolysis as an alternative for targeting energy efficient product distribution

Andres Chico-Proano[a,b], George Manos[a], Lazaros G. Papageorgiou[a] and Eric S. Fraga[a,*]

[a]Department of Chemical Engineering, University College London, Torrington Place, London WC1E 7JE, United Kingdom
[b]Departamento de Ingenieria Quimica, Escuela Politecnica Nacional, Ladron de Guevara E11-253, Quito EC170525, Ecuador
e.fraga@ucl.ac.uk

Energy generation and platform chemicals production from biomass are a potential route towards an oil-free economy. Pyrolysis is one of the key technologies for transforming biomass into both fuels and chemicals. However, pyrolysis is a complex and energy-intensive process, and optimizing the operation for reducing its energy requirements is critical for the design of competitive biorefineries. This work presents a model to describe cellulose pyrolysis based on mass, energy and momentum conservation of solid and gaseous species. Lumped and detailed kinetic models are used to investigate how heating conditions impact pyrolysis product distribution. The resulting complex system was solved using gPROMS. Results suggest that pyrolysis mainly occurs in the boundary of the modelled particles. The developed model presents flexibility to use lumped and detailed kinetic models and provided both a general perspective of the pyrolysis process and detailed information on product distribution. Using this model, the results show that an initial high heating rate, followed by a lower heating rate, could reduce energy requirements by 10 % without changing the product distribution. There is also a trade-off between the yield of high added-value products, such as levoglucosan, and the overall energy requirement.

## 1. Introduction

Biomass has been identified as a renewable resource with potential to facilitate a transition towards an oil-free future economy. Pyrolysis is a key technology for transforming biomass into fuels and diverse platform chemicals with industrial application. In spite of its versatility, pyrolysis is a complex thermo-chemical process and a deeper understanding of the interaction between biomass components, heating rates, and operating conditions is needed for scaling-up and for incorporating pyrolysis into biorefineries (Guedes et al., 2018). Energy consumption is one of the main issues associated with energy-intensive processes such as pyrolysis. Energy efficient pyrolysis needs to be developed, and for such a purpose, a deeper understanding of the interactions between heating and product distribution in pyrolysis is needed (Bridgwater, 2012; Espinoza Pérez et al., 2017).

## 2. Biomass pyrolysis modelling

Biomass pyrolysis is a complex thermo-chemical process that makes use of high temperatures to break long polymeric chains of cellulose, hemicellulose and lignin, into smaller molecules. Within pyrolysis, the existing interactions among feedstocks, intermediate and final products, and by-products, affect the overall yield of the process. Due to the variety of substances involved in biomass pyrolysis, its modelling requires to couple heat and mass transfer to develop applications that could be scaled-up and further integrated into industrial applications (Vinu and Broadbelt, 2012; Ranzi et al., 2014).

In order to model biomass pyrolysis, different reaction schemes could be considered. One such scheme is focused on predicting product composition in terms of its solid (char), liquid (tar) and gaseous (gas) components. The kinetic models that describe pyrolysis under the mentioned three categories are referred to as lumped models (Di Blasi, 2000). However, pyrolysis products, specifically tar (bio-oil), contain many platforms chemicals which cannot be visualized with lumped models. For overcoming such drawback, detailed kinetic models can

be applied. Given the large number of species that detailed models consider, they also have limitations. Such limitations are associated with the necessary trade-off between accuracy of the model and number of intermediate and final species considered (Ranzi et al., 2014; Anca-Couce and Scharler, 2017).

Whenever detailed or lumped models are used, interactions between the different species during pyrolysis need to be considered. For this purpose, single particle models have been used to describe pyrolysis by coupling information from pyrolysis kinetics, heat and mass transfer, and physicochemical properties (Di Blasi, 2000; Anca-Couce and Scharler, 2017; Ranzi et al., 2017a).Through particle models, temperature and product distribution could be predicted. Such models are required whenever a deeper understanding on product distribution and associated energy requirements is needed. Biomass heating during pyrolysis and its effect over product distribution is an area of interest that needs further development. Heating rates of biomass during pyrolysis are critical because they are directly related to product distribution, energy consumption and operation costs (Sharma et al., 2015).

## 3. Cellulose pyrolysis model

A particle and a reactor model for describing cellulose pyrolysis are developed based on energy, mass and momentum conservation of solid and gaseous species. Lumped and detailed kinetic models are applied.

### 3.1 Properties of components and considerations for the model

In order to simplify the analysis, spherical, dry cellulose particles are modelled. During pyrolysis, particles are considered to shrink while maintaining an isometric behavior (Ranzi et al., 2017b) and only the radial variation of properties is taken into account. Only gaseous species are considered to move across the cellulose particle and such gases follow an ideal behavior (Anca-Couce and Zobel, 2012; Debiagi et al., 2016). Local thermal equilibrium between solid and gaseous phases is considered (Shi et al., 2016).

Both lumped and detailed kinetic models from previous works are used to describe cellulose pyrolysis (Di Blasi, 2000; Anca-Couce and Scharler, 2017; Ranzi et al., 2017a). Whereas the lumped kinetic model considers gases, tar and biochar as the only products; the detailed kinetic model includes active cellulose as intermediate product and over 20 different solid, liquid or gaseous products. For the solid and gaseous species, the specific heat capacity ($C_p$) is determined using either a polynomial correlation of $C_p$ with temperature, or an empirical correlation from literature (Dorofeeva et al., 2001). Individual diffusion coefficients are calculated with the Fuller-Schettler-Giddings correlation. Similarly, diffusion coefficients for the gaseous phase are estimated with the Fairbanks and Wilke expression (Anca-Couce and Zobel, 2012).

### 3.2 Pyrolysis models

Both a particle level and a reactor level models are considered to describe pyrolysis. The nomenclature used in the pyrolysis model is presented at the end of this section in Table 1 at the end of this subsection. For the particle model, porosity ($\varphi$) is estimated from biochar ($B$) and cellulose (C) bulk ($\tilde{\rho}$) and initial ($\rho$) densities with Eq(1) (Anca-Couce and Zobel, 2012).

$$\varphi = \frac{(\tilde{\rho}_B + \tilde{\rho}_C)^2}{(\rho_B \tilde{\rho}_B + \rho_C \tilde{\rho}_C)} \quad (1)$$

Mass balances consider the continuity equation for the whole solid phase ($s$) and for each individual component of the solid phase ($s,i$). The mentioned mass balances are calculated from Eq(2) and Eq(3).

$$\varphi = \partial_t[\rho_S(1-\varphi)] = \Gamma_S \quad (2)$$

$$\partial_t[\rho_{S,i}(1-\varphi)] = \Gamma_{S,i} \quad (3)$$

The net formation rate for the solid phase ($\Gamma_S$) is calculated from the contribution of individual solid components ($\Gamma_{S,i}$) with Eq(4) and Eq(5). Reaction rates ($r_j$) are calculated from Eq(6), using the Arrhenius equation and the concentration ($C_{i,j}$) of a specie $i$ as a result of a reaction $j$. Lumped and detailed kinetic parameters and stoichiometric coefficients ($\gamma_{i,j}$) are taken from previous works (Anca-Couce and Zobel, 2012; Ranzi et al., 2014).

$$\Gamma_S = \sum_{i=1}^{n_c} \Gamma_{S,i} \quad (4)$$

***Table 1:*** *Detail of the nomenclature and parameters used in the pyrolysis model*

| | Description | | Description |
|---|---|---|---|
| $A_j$ | pre-exponential factor of reaction *j* ($s^{-1}$) | $\boldsymbol{u}$ | Velocity (m $s^{-1}$) |
| $C_i$ | concentration of component (kg $m^{-3}$) | $w_{G,i}$ | mass fraction of *i* in the gaseous phase |
| $C_p$ | specific heat (J $kg^{-1}K$) | $\Gamma_G$ | net formation of gaseous phase (kg $m^{-3}$ $s^{-1}$) |
| $Ea_j$ | activation energy of reaction *j* (J $mol^{-1}$) | $\Gamma_{G,i}$ | net formation of *i* in the gas phase (kg $m^{-3}$ $s^{-1}$) |
| $h$ | heat transfer coefficient, 20.00 (W $m^{-2}K^{-1}$) | $\Gamma_S$ | net formation of solid phase (kg $m^{-3}$ $s^{-1}$) |
| $j_{G,i}$ | total flux of gas from to diffusion (kg $m^{-1}$ $s^{-1}$) | $\Gamma_{S,i}$ | net formation of *i* in the solid phase (kg $m^{-3}$ $s^{-1}$) |
| $K_S$ | permeability of the solid phase ($m^2$) | $\gamma_{i,j}$ | stoichiometric coefficient of *i* in reaction *j* |
| $k$ | thermal conductivity | $\Delta H_{Rx,j}$ | heat of reaction *j* (J $kg^{-1}$) |
| $n_r$ | number of reactions | $\varepsilon$ | Surface emissivity, 0.90 |
| $n_c$ | number of components | $\tilde{\rho}_B$ | bulk density cellulose (kg $m^{-3}$) |
| P | Pressure (Pa) | $\tilde{\rho}_C$ | bulk density of char (kg $m^{-3}$) |
| R | ideal gas constant (J K $mol^{-1}$) | $\rho_B$ | initial density of cellulose (kg $m^{-3}$) |
| $R_{particle}$ | particle radius at a given time (m) | $\rho_C$ | initial density of char (kg $m^{-3}$) |
| $r_j$ | reaction rate for reaction j (kg $m^{-3}$ $s^{-1}$) | $\rho_G$ | apparent density of gaseous phase (kg $m^{-3}$) |
| $T$ | Temperature (K) | $\rho_S$ | apparent density of the solid phase (kg $m^{-3}$) |
| $T_0$ | Initial temperature (K) | $\rho_{S,i}$ | apparent density of *i* in solid phase (kg $m^{-3}$) |
| $T_R$ | temperature at r = $R_{particle}$ (K) | $\rho_f$ | density of the gaseous-solid phase (kg $m^{-3}$) |
| $T_\infty$ | temperature outside the particle (K) | $\sigma$ | $5.67 \cdot 10^{-8}$ (W $m^{-2}K^{-4}$) |
| $t$ | time (s) | $\varphi$ | porosity |

$$\Gamma_{S,i} = \sum_{j=1}^{n_r} \gamma_{i,j} r_j \tag{5}$$

$$r_j = A_j e^{-\frac{Ea_j}{RT}} C_{i,j} \tag{6}$$

The gaseous phase mass balance is calculated from Eq(7). The gaseous mixture moves across the solid particle with a velocity ($\boldsymbol{u}$) and the momentum transfer could be described using the Darcy Law in Eq(8).

$$\partial_t(\rho_G \varphi) = -\nabla \cdot (\rho_G \boldsymbol{u}) + \Gamma_G \tag{7}$$

$$\boldsymbol{u} = -\frac{K_S}{\varphi \mu_G} \nabla P \tag{8}$$

Individual gas mass balances inside the particle ($_{G,i}$) are calculated from Eq(9). Individual gas fluxes through the particle ($\boldsymbol{j}_{G,i}$) is calculated with the effective diffusivity ($D_{\mathrm{eff},i}$) from Eq(10) (Anca-Couce and Zobel, 2012).

$$\partial_t\left(\rho_G \varphi w_{G,i}\right) = -\nabla \cdot \left(\rho_G \varphi w_{G,i} \boldsymbol{u}\right) - \nabla \cdot \boldsymbol{j}_{G,i} + \Gamma_{G,i} \tag{9}$$

$$\boldsymbol{j}_{G,i} = -D_{\mathrm{eff},i} \nabla \rho_G \varphi w_{G,i} \tag{10}$$

The energy balance is presented in Eq(11). Average specific heats for the solid $\langle C_{PS} \rangle$ and gaseous $\langle C_{PG} \rangle$ phases are used. The heat of reaction and thermal conductivities are included in the $\boldsymbol{q}$ term.

$$(\rho_S \varphi \langle C_{PS} \rangle + \rho_G (1-\varphi) \langle C_{PG} \rangle) \frac{DT}{Dt} = -\nabla \cdot \boldsymbol{q} - \left(\frac{\partial \ln \rho_G}{\ln T}\right)_P \frac{DP}{Dt} \tag{11}$$

Boundary conditions for the mentioned energy equation are presented in Eq(12) and Eq(13).

$$\partial_r T|_{r=0} = 0 \tag{12}$$

$$k \partial_r T|_{r=R} = -h(T_R - T_\infty) - \sigma \varepsilon ({T_R}^4 - {T_\infty}^4) \tag{13}$$

For comparison purposes, a simplified adiabatic plug flow reactor (PFR) is developed. The reactor model neglects radial and axial diffusion without the particle approach. In such circumstances, and considering average properties for solid and gaseous phases, the mass and energy balances can be represented with Eq(14) and Eq(15). The mentioned models, consisting of a set of ODEs, DEs and algebraic equations, are solved using

gPROMS ModelBuilder® version 5.1.1. The novelty of the model relates to the use of lumped and detailed kinetic models, to the application of boundary immobilization and to the possibility of including information regarding changing heating rates (Anca-Couce and Zobel, 2012; Ranzi et al., 2014; Christodoulou et al., 2017).

$$\partial_t C_i = -v\partial_z C_i + \sum_{j=1}^{n_r} \gamma_{ij} r_j \tag{14}$$

$$\rho_f \langle C_{Pf} \rangle \partial_t T = -\rho_f \langle C_{Pf} \rangle \partial_z T + \sum_{j=1}^{n_r} r_j \left(-\Delta H_{Rx,j}\right) \tag{15}$$

## 4. Results and discussion

As it is presented in Figure 1 the yield of levoglucosan (LVG) from the PFR model does not match the experimental values found in literature for the evaluated temperatures. The difference between experimental and PFR modeled LVG yields is 73 % for 450 °C and 45 % for 550 °C. In contrast, LVG yields from the particle model (Figure 1b) provide a better match with the yields found in literature. A similar behavior was observed for the other products from pyrolysis. This difference between the models could be explained by considering that the simplifications made for the PFR model do not allow to capture the pyrolysis process when products interact between each other. By considering a particle scale, interactions between products at every phase are described more accurately (Sengar et al., 2019). Consequently, approaching pyrolysis from a particle model point of view, instead of a bulk PFR reaction perspective might provide a better representation of the process.

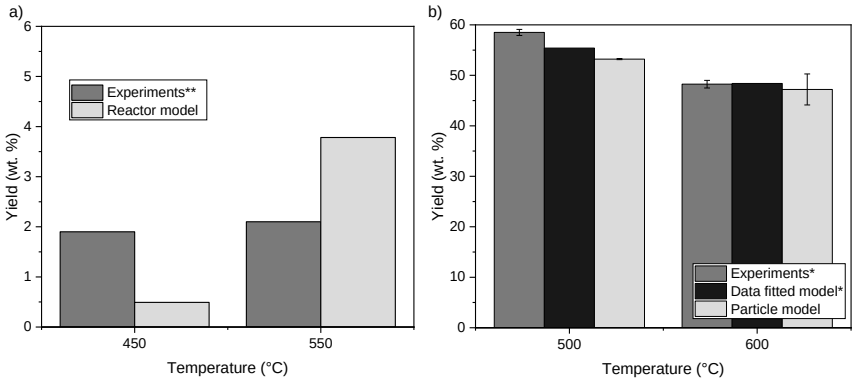


*Figure 1: Levoglucosan yields from the developed models and literature. a) PFR reactor model for fast pyrolysis, residence time= 0.53, **(Radlein et al., 1991). b) Particle model, r= 9·10$^{-3}$ m, $T_0$= 250 °C and $T_\infty$= 800 °C, considering average yields. *Experimental and fitted data from literature* (Vinu and Broadbelt, 2012).

The particle model shows that cellulose particles mainly react in the proximities of their boundary for short reaction times during pyrolysis. The mentioned behaviour (Figure 2a), could be explained when biomass low thermal conductivity and porosity is considered. Consequently, pyrolysis will most likely occur in regions of higher temperature, closer to the surface of the particle. The tendency of cellulose decomposition evidenced in Figure 2b (fast decomposition in short time), corresponds with cellulose thermal decomposition during thermo gravimetric analysis (Várhegyi et al., 1997).

The results presented in Figure 3, show that temperature affects product distribution from cellulose pyrolysis, both for lumped and for detailed kinetic schemes. Whereas the lumped model provided a straightforward understanding of the effect of temperature over product distribution, the detailed model makes it possible to visualize pyrolysis valuable products. For instance, in Figure 3b, for 650 °C and 750 °C the fraction of the gaseous phase is similar (0.38 and 0.42); however, the fraction of levoglucosan reduces in more than 60 % for the same temperatures. This reduction could not have been spotted with lumped models. Consequently, whereas lumped models could be useful for applications where little detail on the products is needed, for instance energy applications; detailed particle models could support future decision-making processes when both platform chemicals and energy are required.

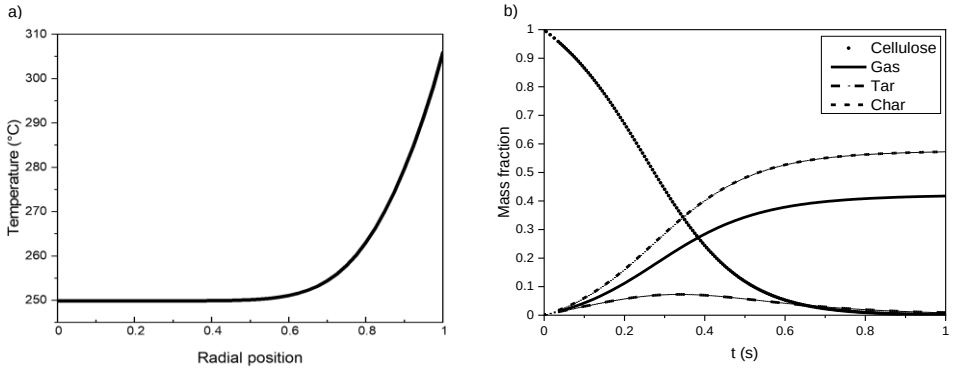


*Figure 2: a) Temperature gradient during pyrolysis for particles of $5 \cdot 10^{-3}$m of diameter after 5 s and $T_0$= 250 °C, from the centre (0.0) to the border (1.0). b) Distribution of lumped products for cellulose pyrolysis at 650 °C.*

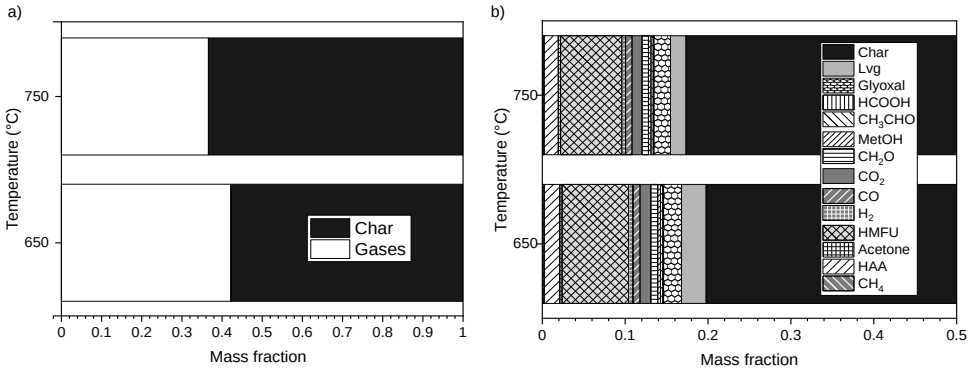


*Figure 3: Distribution of products from cellulose pyrolysis with the particle model for different pyrolysis temperatures (650 °C and 750 °C) considering: a) lumped kinetic models and b) detailed kinetic models.*

### 4.1 Application of the particle model to evaluate heating strategies

To evaluate pyrolysis energy requirements, and to visualize changes in composition associated with heating, 4 heating alternatives were considered: a constant heating rate with a low heat flux $\dot{Q}_1$ (Alternative 1), a higher heat flux $\dot{Q}_2 > \dot{Q}_1$ (Alternative 2), a combination in order $\dot{Q}_1 + \dot{Q}_2$(Alternative 3), and finally, a combination in order $\dot{Q}_2 + \dot{Q}_1$ (Alternative 4). The combination of $\dot{Q}_2$ and $\dot{Q}_1$considered equal intervals of time in each case.

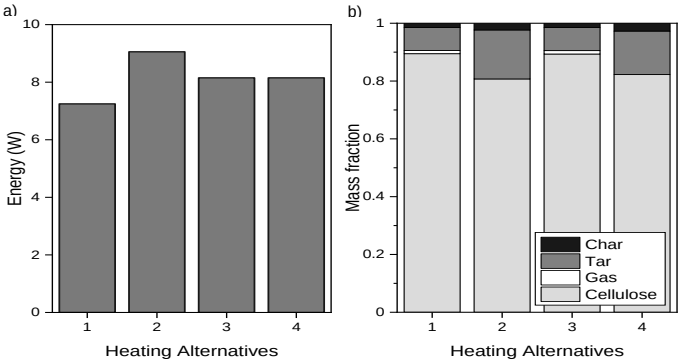


*Figure 4. Energy consumption for different heating alternatives a) and the corresponding product distribution b).*

Figure 4 shows that increasing the heat flux for a single particle results into higher tar concentrations. Figure 4 also shows that different heating strategies can give similar product distributions. Moreover, Figures 4a and 4b suggest that the initial heating rate determines the product distribution for lumped models. Results show that heating alternatives 1 and 3 result into similar product distribution even if they have different energy

requirements. Similarly, if a high tar content is needed, alternatives 2 and 4 could be used. In such case, combining heating strategies (alternative 4) has the potential to reduce the energy requirements associated to pyrolysis in approximately 10 %. The mentioned behavior opens a future possibility for addressing process optimization, from a particle level scale, with views to minimize the associated energy requirements.

## 5. Conclusions

A model to describe cellulose pyrolysis has been developed based on mass, energy and momentum conservation of the involved solid and gaseous species. The developed model predicts temperature and composition in a shrinking cellulose particle. For the modelled particle sizes, reaction mainly takes place in the shrinking boundary of the particle. The model presents flexibility to use both lumped and detailed pyrolysis reaction schemes. Finally, different heating strategies can potentially reduce pyrolysis energy requirements nearly by 10 %, and they could be used as a starting point for process optimization at particle and reactor scales.

**Acknowledgments**

Secretaría de Educación Superior, Ciencia, Tecnología e Innovación-SENESCYT Ecuador.

**References**

Anca-Couce, A., Scharler, R., 2017, Modelling heat of reaction in biomass pyrolysis with detailed reaction schemes, Fuel, 206, 572–579.

Anca-Couce, A., Zobel, N., 2012, Numerical analysis of a biomass pyrolysis particle model: Solution method optimized for the coupling to reactor models, Fuel, 97, 80–88.

Bridgwater, A.V., 2012, Review of fast pyrolysis of biomass and product upgrading, Biomass and Bioenergy, 38, 68–94.

Christodoulou, C., Mazzei, L., García-Muñoz, S., Sorensen, E., 2017, Modelling of Droplet Absorption and Evaporation during Pharmaceutical Tablet Coating, Computer Aided Chemical Engineering, 40, 85–90.

Debiagi, P., Gentile, G., Pelucchi, M., Frassoldati, A., Cuoci, A., Faravelli, T., Ranzi, E., 2016, Detailed kinetic mechanism of gas-phase reactions of volatiles released from biomass pyrolysis, Biomass and Bioenergy, 93, 60–71.

Di Blasi, C., 2000, Modelling the fast pyrolysis of cellulosic particles in fluid-bed reactors, Chemical Engineering Science, 55(24), 5999–6013.

Dorofeeva, O., Novikov, V., Neumann, D., 2001, NIST-JANAF thermochemical tables. I. Ten organic molecules related to atmospheric chemistry, Journal of Physical and Chemical Reference Data, 30(2), 475–509.

Espinoza Pérez, A., Camargo, M., Narváez Rincón, P., Alfaro Marchant, M., 2017, Key challenges and requirements for sustainable and industrialized biorefinery supply chain design and management: A bibliographic analysis, Renewable and Sustainable Energy Reviews, 69, 350–359.

Guedes, R.E., Luna, A.S., Torres, A.R., 2018, Operating parameters for bio-oil production in biomass pyrolysis: A review, Journal of Analytical and Applied Pyrolysis, 129, 134–149.

Radlein, D., Piskorz, J., Scott, D.S., 1991, Fast pyrolysis of natural polysaccharides as a potential industrial process, Journal of Analytical and Applied Pyrolysis, 19, 41–63.

Ranzi, E., Corbetta, M., Manenti, F., Pierucci, S., 2014, Kinetic modeling of the thermal degradation and combustion of biomass, Chemical Engineering Science, 110, 2–12.

Ranzi, E., Debiagi, P., Frassoldati, A., 2017a, Mathematical Modeling of Fast Biomass Pyrolysis and Bio-Oil Formation. Note I: Kinetic Mechanism of Biomass Pyrolysis, ACS Sustainable Chemistry and Engineering, 5(4), 2867–2881.

Ranzi, E., Debiagi, P., Frassoldati, A., 2017b, Mathematical Modeling of Fast Biomass Pyrolysis and Bio-Oil Formation. Note II: Secondary Gas-Phase Reactions and Bio-Oil Formation, ACS Sustainable Chemistry and Engineering, 5(4), 2882–2896.

Sengar, A., Kuipers, J. A. M., van Santen, R. A., Padding, J. T. (2019). Towards a particle based approach for multiscale modeling of heterogeneous catalytic reactors. Chemical Engineering Science, 198, 184–197.

Sharma, A., Pareek, V., Zhang, D., 2015, Biomass pyrolysis - A review of modelling, process parameters and catalytic studies, Renewable and Sustainable Energy Reviews, 50, 1081–1096.

Shi, X., Ronsse, F., Pieters, J.G., 2016, Finite element modeling of intraparticle heterogeneous tar conversion during pyrolysis of woody biomass particles, Fuel Processing Technology, 148, 302–316.

Várhegyi, G., Antal, M., Jakab, E., Szabó, P., 1997, Kinetic modeling of biomass pyrolysis, Journal of Analytical and Applied Pyrolysis, 42(1), 73–87.

Vinu, R., Broadbelt, L.J., 2012, A mechanistic model of fast pyrolysis of glucose-based carbohydrates to predict bio-oil composition, Energy and Environmental Science, 5(12), 9808–9826.